attraction (E_B) associated with the binding of the charged bipolaron to the counterion[5b,6] are included, the two bipolaron transitions satisfy the following relation:

$$\hbar\omega_1 + \hbar\omega_2 = E_{\pi\pi^*} - 2(U_B - E_B)$$

where U_B is the difference in the Coulomb energy between initial state (double charge) and final state (single charge). Since $\hbar\omega_1 + \hbar\omega_2 \approx 2.05$ eV, $U_B \approx E_B$. The resulting values are nearly identical with those obtained for polythiophene.[5,6] Thus, as for polythiophene, the spectroscopic data for P3HT in dilute solution imply relatively weak Coulomb interactions.

The implied change in local conformation in the vicinity of the bipolaron provides an explanation for the excess absorption near 2.15 eV in the doped samples. If the doping-induced straight-chain region extends somewhat beyond the coherence length of the bipolaron, doping would shift oscillator strength from the π–π^* transition of the neutral polymer in solution to near that of the neutral straight chain, in agreement with the experimental results.

Summary and Conclusion

In summary, we find that the spinless bipolaron is the lowest energy charge-storage configuration on single P3HT macromolecules in dilute solution. Polarons are formed either as a result of an odd number of charges on a single polymer chain or as a result of interchain interactions (in the semidilute regime). The conclusion that the bipolaron is the lowest energy charge-storage configuration together with the results of detailed analysis of the absorption spectra indicate that electron–electron Coulomb correlations are relatively weak, even for isolated conducting polymer chains in dilute solution. More generally, the results demonstrate that the novel concepts developed in the study of the solid-state properties of conducting polymers are directly applicable to such polymers in solution.

Acknowledgment. We thank N. Colaneri for generously helping with the absorption spectra and for discussions of the implications of these data. We are grateful to Prof. F. Wudl for making facilities available for sample preparation and characterization and to Dr. R. H. Friend for comments and discussions. This research was supported in part by the Office of Naval Research; the ESR studies were supported by the National Science Foundation (DMR 85-21392).

Registry No. P_3HT, 104934-50-1; $(NO)^+(PF_6)^-$, 16921-91-8.

References and Notes

(1) (a) Skotheim, T. J., Ed. *Handbook of Conducting Polymers*; Marcel Dekker: New York, 1986. (b) Etemad, S.; Heeger, A. J.; MacDiarmid, A. G. *Annu. Rev. Phys. Chem.* **1982**, *33*, 443. (c) Bredas, J. L.; Street, G. B. *Acc. Chem. Res.* **1985**, *18*, 309.
(2) (a) Su, W. P.; Schrieffer, J. R.; Heeger, A. J. *Phys. Rev. Lett.* **1979**, *42*, 1698; *Phys. Rev. B: Condens. Matter* **1980**, *22*, 2099. (b) Schrieffer, J. R. *Highlights of Condensed Matter Theory*; Society Italiana di Fisica: Bologna, 1985. (c) Rice, M. J. *Phys. Lett. A* **1979**, *71A*, 152. (d) Takayama, H.; Lin-Liu, Y. R.; Maki, K. *Phys. Rev. B: Condens. Matter* **1980**, *21*, 2388.
(3) (a) Brazovskii, S. A.; Kirova, N. *JETP Lett.* **1981** *33*, 4. (b) Campbell, D. K.; Bishop, A. R. *Phys. Rev. B: Condens. Matter* **1981**, *24*, 4859; *Nucl. Phys. B* **1982**, *200*, 297.
(4) (a) Heeger, A. J. *Comments Solid State Phys.* **1981**, *10*, 53. (b) Lauchlan, L.; Etemad, S.; Chung, T.-C.; Heeger, A. J.; MacDiarmid, A. G. *Phys. Rev. B: Condens. Matter* **1981**, *29*, 3701.
(5) (a) Chung, T.-C; Kaufman, J. H.; Heeger, A. J.; Wudl, F. *Phys. Rev. B: Condens. Matter* **1981**, *30*, 702. (b) Chen, J.; Heeger, A. J. *Solid State Commun.* **1986**, *58*, 251.
(6) Vardeny, Z.; Ehrenfreund, E.; Brafman, O.; Nowak, M.; Schaffer, H.; Heeger, A. J.; Wudl, F. *Phys. Rev. Lett.* **1986**, *56*, 671.
(7) (a) Harbeke, G.; Meier, E.; Kobel, W.; Egli, M.; Kiess, H.; Tosatti, E. *Solid State Commun.* **1985**, *55*, 419. (b) Kaneto, K.; Kohno, Y.; Yoshino, K. *Solid State Commun.* **1984**, *51*, 267. (c) Genoud, F.; Guglielmi, M.; Nechtschein, M.; Genies, E.; Salmon, M. *Phys. Rev. Lett.* **1985**, *55*, 118.
(8) Jen, K. Y.; Oboodi, R.; Elsenbaumer, R. L. *Polym. Mater Sci. Eng.* **1985**, *53*, 79; *Synth. Met.* **1986**, *15*, 169.
(9) Hotta, S.; Rughooputh, S. D. D. V.; Heeger, A. J.; Wudl, F. *Macromolecules* **1987**, *20*, 212.
(10) Sato, M.; Tanaka, S.; Kaeriyama, K. *Chem. Commun.* **1986**, 873.
(11) The doping-induced spectral changes for P3HT in solution at c_0 saturate with no additional shifts in oscillator strength above a nominal y of about 0.5. Since the maximum charge storage in thin films is about one per two to three rings, we infer that the actual doping level is close to the nominal level.
(12) Moraes, F.; Chen, J.; Chung, T.-C.; Heeger, A. J. *Synth. Met.* **1985**, *11*, 271. Moraes, F.; Davidov, D.; Kobayashi, M.; Chung, T.-C.; Chen, J.; Heeger, A. J.; Wudl, F. *Synth. Met.* **1985**, *10*, 169.
(13) Carrington, A.; McLachlan, A. *Introduction to Magnetic Resonance*; Harper and Row: New York, 1967. The hyperfine splitting is 22.5 G per spin for C_6H_6 and 29.9 G per spin for C_5H_5.
(14) See ref 1c and references therein.
(15) Saxena, A.; Gunton, J. D., preprint.
(16) Rughooputh, S. D. D. V.; Hotta, S.; Heeger, A. J.; Wudl, F. *J. Polym. Sci., Polym. Phys. Ed.*, in press.
(17) Colaneri, N., to be published.
(18) Sato, M.-A.; Tanaka, S.; Kaeriyama, K. *Synth. Met.* **1986**, *14*, 289.

Protonic Conduction in Poly(ethylenimine) Hydrates

Masayoshi Watanabe,* Ryoichi Ikezawa, Kohei Sanui, and Naoya Ogata*

Department of Chemistry, Sophia University, 7-1 Kioi-cho, Chiyoda-ku, Tokyo 102, Japan.
Received September 9, 1986

ABSTRACT: The ionic conductivity of crystalline hydrates of linear poly(ethylenimine) (PEI) was investigated as a function of temperature and water content. The main carriers were likely protons. The temperature dependence of the ionic conductivity obeyed the Arrhenius equation, and the activation energies were 18–20 kcal/mol irrespective of the composition of the hydrates. The ionic conductivity reached 10^{-5} S cm^{-1} at 30 °C in the hydrate with $[H_2O]/[EI\ unit] = 1.5$. A comparison to the conducting behavior of partially amorphous PEI hydrates, which were made by a cross-linking reaction, suggested that the ionic conduction in the linear PEI hydrates occurred in the crystalline phases and that the network structure of hydrogen bonds played an important role in the ionic conduction.

Introduction

The study of ionic conductivity of polymers is of considerable significance in terms of the fundamental understanding of dynamic process proceeding within polymers and of the major functions of energy storage and conversion. Studies have been performed on various kinds of ion-containing polymers in the presence and absence of solvents. An example of the former is highly protonic

0024-9297/87/2220-0968$01.50/0

Scheme I

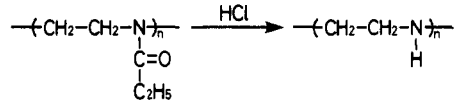

conduction in hydrated ion-exchange membranes,[1] although conductivity of dried membranes is very low.[2,3] For instance, hydrated perfluorosulfonic acid membranes, commercially called Nafion by E. I. Du Pont Co., show protonic conductivity of the order of 10^{-2} S cm^{-1} at room temperature.[4,5] An example of the latter is polymer complexes consisting of poly(ethylene oxide) and alkali metal salts.[6] In both cases, carrier ions migrate primarily in the amorphous region of these ion-containing polymers. Thus, ion transport in the former and latter cases seems to be limited by the microviscosity[7] and segmental mobility[8-10] around the carrier ions, respectively, which may prohibit much higher ionic conductivity in polymeric materials.

Certain kinds of crystalline inorganic solids, typically Ag_4RbI_5 and sodium β-alumina, show high ionic conductivities of 10^{-1}–10^{-2} S cm^{-1} at moderate temperatures.[11] The high ionic conductivity is attained by the special crystal structures which allow fast ion-transport.[11] However, no experimental evidence of fast ion transport in crystalline phases of polymers has been put forth so far, to our knowledge.

In this study, our attention has been directed to linear poly(ethylenimine) (PEI).[12-14] It has been revealed that PEI forms three kinds of hydrated crystals, that is, hemihydrate,[15] sesquihydrate,[16] and dihydrate.[16] In these hydrates, two-dimensional (hemihydrate) and three-dimensional (sesquihydrate and dihydrate) networks of hydrogen bonds are formed. It is well-known that most crystalline proton conductors with high conductivity have a network structure of hydrogen bonds, in which cooperative proton transfer occurs.[17] Thus, we considered that PEI hydrates could be a model of crystalline ionic conductors based on polymeric materials. The ionic conductivity of the crystalline hydrates was investigated as a function of temperature and water content. Carrier ions were demonstrated to be protons. The structure and conductivity relationships were discussed, in contrast to those in partially amorphous PEI hydrates which were made by a cross-linking reaction.

Experimental Section

Poly(ethylenimine) Anhydrate. PEI was prepared by a hydrolysis reaction of poly(ethyloxazoline) (PEOX) in the presence of hydrochloric acid,[13] according to Scheme I. PEOX with a weight-average molecular weight of 5×10^5 was kindly provided by Dow Chemical Co. and used without further purification. PEOX (40 g) was dissolved in a mixture of pure water (380 mL) and concentrated hydrochloric acid (600 mL), and was refluxed for 5 days. Upon reaction, the reaction solution gradually became turbid. After the reaction, hydrochloride gas was evaporated through a rotary evaporator. The reaction mixture was poured into a large excess of methanol to yield white precipitates (PEI hydrochloride), which were filtered off and washed with methanol several times in order to exclude the byproduct of propionic acid. The precipitates were dissolved again in pure water, and an aqueous solution of sodium hydroxide was added dropwise with stirring till the solution became slightly basic. Near the neutralization point white precipitates formed. The precipitates were filtered off and washed with cold pure water until the filtrate became neutral and chloride ion was not detected by a 0.1 N $AgNO_3$ aqueous solution. The crude PEI hydrates were recrystallized twice from ethanol and dried under vacuum at 100 °C for 24 h to yield massive PEI anhydrate. The massive PEI anhydrate was crushed finely in an argon-filled drybox. The average molecular weight, without taking account of chain scission during the hydrolysis, was 2.7×10^5: mp 45 °C; IR 3260 (ν_{NH}), 2900, 2850 (ν_{CH_2}), 1470 (δ_{CH_2}), 1130 cm^{-1} (ν_{CN}); ^{1}H NMR ($CDCl_3$) δ 1.57 (s, 1 H, NH), 2.70 (s, 4 H, CH_2).

Scheme II

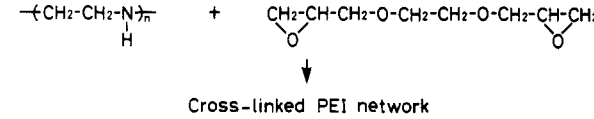

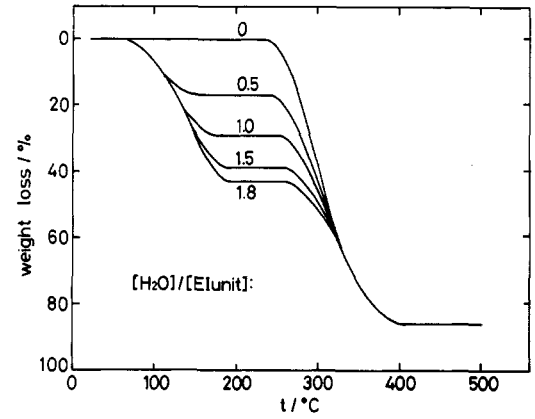

Figure 1. TGA curves for the linear poly(ethylenimine) anhydrate and hydrates.

Poly(ethylenimine) Hydrates. Powdered PEI anhydrate was allowed to stand in desiccators under 100% relative humidity at room temperature. After an appropriate period, several kinds of PEI hydrates could be obtained. The standing periods were several hours for preparing hemihydrate and a few days for sesqui- and dihydrates. The composition of the hydrates was determined thermogravimetrically and was represented by the molar ratio of water to the repeat unit of PEI ([H_2O]/[EI unit]).

Cross-Linked Poly(ethylenimine). In order to make partially amorphous PEI, cross-linked PEI networks were prepared according to Scheme II. A given amount of PEI anhydrate was dissolved in anhydrous chloroform, and 1 molar amount of distilled ethylene glycol diglycidyl ether toward 6 EI units was added. The total precursor concentration was 10 wt %. The mixed solution was cast on a glass substrate, and chloroform was allowed to evaporate at room temperature under nitrogen gas flow. A cross-linking reaction occurred at 70 °C for 48 h under nitrogen atmosphere. Unreacted precursors were extracted several times by chloroform. The films obtained were dried under vacuum at 70 °C for 72 h. Hydrated films were also prepared according to the method described above.

Measurements. Electrical measurements were performed on pressed cylindrical pellets (10-mm diameter, ~0.5-mm thickness) for linear PEI hydrates and on disk films (13-mm diameter, ~0.2-mm thickness) for hydrated PEI networks. Electrodes used were platinum or WO_3. Anhydrous WO_3 (Furuuchi Kagaku Co., 99.99%) was evaporated onto stainless steel disks or transparent conducting substrates (indium tin oxide (ITO) on glass, surface resistance <30 Ω) under a reduced pressure lower than 5×10^{-5} Torr and were used as WO_3 electrodes.

The sample sandwiched between two electrodes was packed in a sealed cell made of poly(tetrafluoroethylene) with stainless steel terminals, which were connected to the measuring device. The dead volume in the cell was negligible. The cell impedance was measured with a Yokogawa-Hewlett-Packard 4192 LF-impedance analyzer over a frequency range of 5 to 1×10^6 Hz.

Differential scanning calorimetry (DSC) and thermogravimetrical analysis (TGA) were performed with Rigaku DSC and TGA apparatus, respectively, at a heating rate of 20 °C/min. In both measurements, a hydrated sample was packed in a pan with a cover having a pinhole in order to allow dehydration. Powder X-ray diffraction patterns were recorded by using a Rigaku RAD-IIA diffractometer. The radiation used was Ni-filtered Cu Kα. Electronic spectra of WO_3-evaporated ITO–glass substrates, before and after polarization experiments, were measured with a Shimazu UV-240 spectrophotometer.

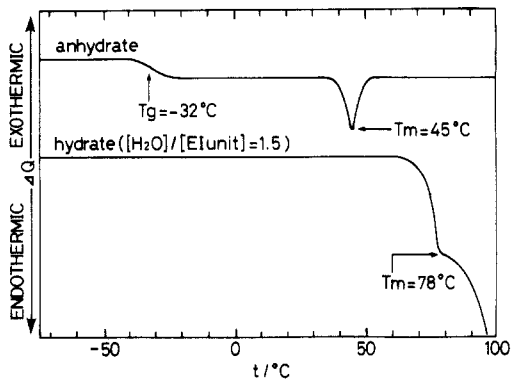

Figure 2. Profiles of DSC curves for the linear poly(ethylenimine) anhydrate and a typical hydrate.

Results and Discussion

Thermal and X-ray Analysis. Figure 1 shows TGA curves of PEI anhydrate and PEI hydrates with various water content. PEI anhydrate began to loose weight at about 250 °C and lost 85% of the initial weight at 400 °C. This weight decrease corresponded to decomposition of PEI. Weight loss against temperature for various kinds of hydrates showed two step profiles. The first weight loss started at 70 °C, and the second one started at about 250 °C. Since the temperature of the second weight loss coincided with that of anhydrate, the first weight loss corresponded to dehydration of the hydrates. From the first weight loss, compositions of the hydrates were determined.

Profiles of DSC curves for the anhydrate and a typical hydrate ($[H_2O]/[EI\ unit] = 1.5$) are shown in Figure 2. PEI anhydrate was very hygroscopic and turned inevitably to the mixture of anhydrate and trace hemihydrate during the sample preparation for DSC measurements. Thus, the first run of the DSC curve of PEI anhydrate showed three endothermic peaks at 52, 74, and 138 °C, which corresponded to melting temperatures (T_m) of the anhydrate and hemihydrate and the dehydration temperature, respectively. The DSC curve in Figure 2 was the trace of second run, after raising the temperature of the partial hydrate up to 200 °C and cooling to −150 °C at 5 °C/min in the DSC apparatus. From the thus-obtained DSC curve, it was found that the glass transition temperature (T_g) and T_m of the anhydrate were −32 and +45 °C, respectively. The DSC curves of the hydrates did not show a glass transition irrespective of the compositions, and T_m ranged from 70 to 80 °C. Since the melting peaks of the hydrates were superposed by large endothermic peaks due to dehydration, the T_m of the hydrates appeared as shoulders. However, it was confirmed that these shoulders corresponded to T_m with the assistance of microscopic measurements. By the inclusion of water to the anhydrate, T_m increased by 25–35 °C. There was no transition corresponding to the melting of water between −150 °C and T_m. This indicated that all of the incorporated water formed hydrogen bonds with water itself or with NH groups of PEI and existed as "crystallized water". Furthermore, the increase in T_m of the hydrates compared with T_m of the anhydrate suggested that the structures of crystalline hydrates were stabilized by strong hydrogen bonds.

Figure 3 shows X-ray diffraction patterns of PEI anhydrate and various kinds of hydrates. The diffraction patterns changed drastically depending on the water content. The anhydrate showed intense diffraction peaks at 2θ = 11.5°, 20.3°, and 23.8°. In the hemihydrate ($[H_2O]/[EI\ unit] = 0.5$) the peak at 2θ = 11.5° disappeared and new peaks at 2θ = 18.3° and 27.6° appeared. Intense

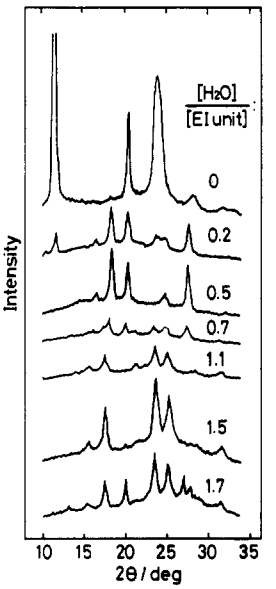

Figure 3. X-ray diffraction patterns of the linear poly(ethylenimine) anhydrate and hydrates.

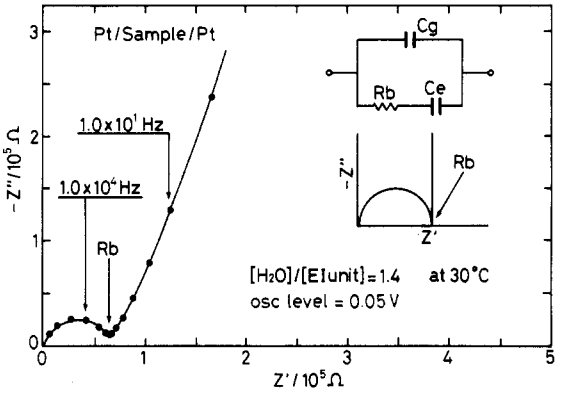

Figure 4. Complex impedance spectrum of linear poly(ethylenimine) hydrate sandwiched between platinum electrodes and corresponding equivalent circuit: C_g, geometrical capacitance; R_b, bulk resistance; C_e, electrode/electrolyte interfacial capacitance.

peaks at 2θ = 17.5°, 23.6°, and 25.1° were observed in the sesquihydrate ($[H_2O]/[EI\ unit] = 1.5$). The change in the diffraction patterns and the peak positions coincided well with those reported by Chatani et al.[15] When the water content of a PEI hydrate was between that of these crystalline phases, the hydrate was considered to be a mixture of the two crystalline hydrates with a composition nearest to the hydrate.[15] Thus, crystal structures of PEI and its hydrates changed in accordance with the water content. The degree of crystallinity of these hydrates is not clear. However, the diffraction patterns of a certain hydrate in this study, whose composition was determined by TGA, were the same as those reported in the literature,[15] where the composition was determined by X-ray structure analysis. Thus, we considered that the fraction of amorphous region was negligible in these hydrates. The absence of T_g and the endothermic peaks due to the T_m of water also supported this consideration.

Ionic Conductivity of PEI Hydrates. In order to exclude electrode processes, such as electrode polarization, from bulk resistance of the sample, we measured the complex impedance of the sample with different kinds of electrodes. Figures 4 and 5 show typical complex impedance spectra of a hydrate with platinum and WO_3 electrodes, respectively. Platinum and WO_3 were expected to

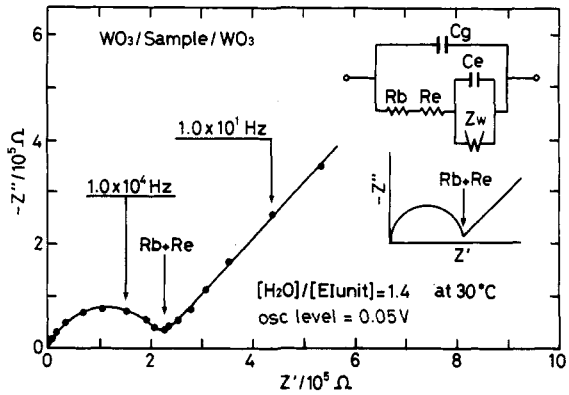

Figure 5. Complex impedance spectrum of linear poly(ethylenimine) hydrate sandwiched between WO_3 electrodes and corresponding equivalent circuit: C_g, R_b, and C_e have the same meanings as in Figure 4; R_e, charge-transfer resistance; Z_w, Warburg impedance.

act as blocking and nonblocking electrodes to a protonic conductor, respectively. The main difference in the two spectra was the low-frequency behavior, which corresponded to electrode processes. The profile of the spectrum in Figure 4 could be interpreted by the equivalent circuit assuming an ideally blocking nature of platinum electrodes, as shown in the figure. In contrast, the slope of the low-frequency impedance locus in the WO_3 electrode cell was 45° from the Z' axis. This profile has been observed in a WO_3/proton-conducting solution system,[18] and an equivalent circuit interpreting the impedance behavior has been proposed by Randin et al.,[18] as shown in Figure 5. The Warburg impedance (Z_w) in the equivalent circuit can be written

$$Z_w = k\omega^{-1/2}(1 - i)$$

where k is a constant, ω is the angular frequency, and i is the imaginary unit and expresses a diffusion-controlled electrode process. Randin et al.[18] concluded that Z_w in their system corresponded to the diffusion of the proton in WO_3 layer. Thus, this impedance profile in our system might correspond to the diffusion of the proton in the WO_3 layer by analogy to the above system and might imply that the proton was a charge carrier in PEI hydrates. The Z' values at the low-frequency ends of the high-frequency arcs were somewhat larger in the WO_3 electrode cell. This was due to the fact that the Z' value in the platinum electrode cell coincided with the bulk resistance (R_b) of the hydrate, whereas that in the WO_3 electrode cell coincided with the sum of R_b and the charge-transfer resistance (R_e), as shown in Figures 4 and 5. The R_b values of a platinum electrode cell were independent of the oscillation levels of ac voltage between 5×10^{-3} and 5×10^{-1} V, from which the conductivity of the PEI hydrates was calculated.

In order to demonstrate more directly species of carrier ions, PEI hydrates sandwiched between WO_3-evaporated ITO–glass plates were polarized at 0.05 V for 1 h, and the change in the electronic spectra of the electrodes before and after the polarization was investigated. Before the polarization both the WO_3 electrodes were colorless (pale yellow). After the polarization all the cathode surface in contact with a PEI hydrate turned purple, while the color of the anode did not change. Figure 6 shows the change in electronic spectra. After the polarization absorbance at around 800 nm increased. It is known that WO_3 reacts electrochemically with such cations (M^+) as H^+,[19,20] Li^+,[21] and Ag^+[22] and forms colored M_xWO_3. Since in PEI hydrates only H^+ can react with WO_3, the electrochemical reaction shown in Figure 6 was considered to occur. Thus,

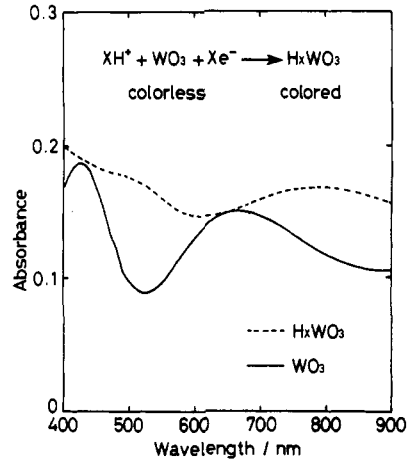

Figure 6. Change in electronic spectra of WO_3 cathodes before and after polarization.

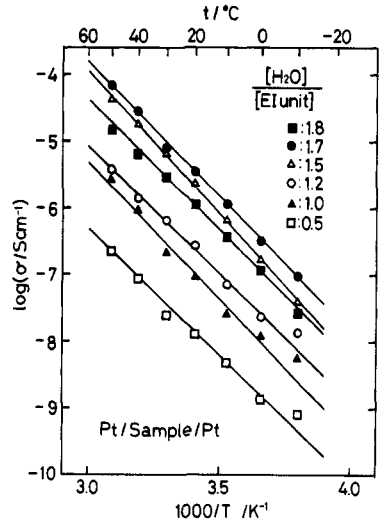

Figure 7. Arrhenius plots of ionic conductivity for linear poly(ethylenimine) hydrates.

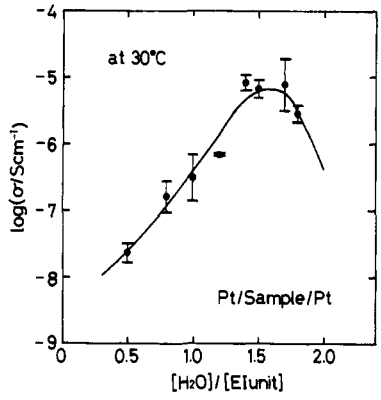

Figure 8. Ionic conductivity of linear poly(ethylenimine) hydrates at 30 °C as a function of water content.

it was demonstrated that the proton was a charge carrier in PEI hydrates.

Figure 7 shows the Arrhenius plots of ionic conductivity for PEI hydrates. The profiles of the Arrhenius plots were linear irrespective of the water content. The activation energy that was determined from the slopes of the plots was independent of the composition and ranged from 18 to 20 kcal/mol. This implied that the carrier conduction in PEI hydrates occurred by the hopping mechanism. The drastic change in the conductivity at 0 °C was not ob-

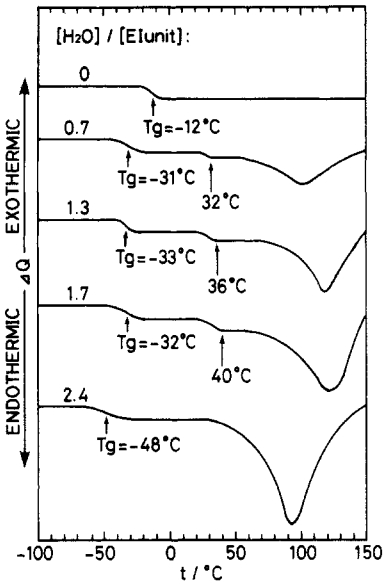

Figure 9. Profiles of DSC curves for cross-linked poly(ethylenimine) anhydrate and hydrates.

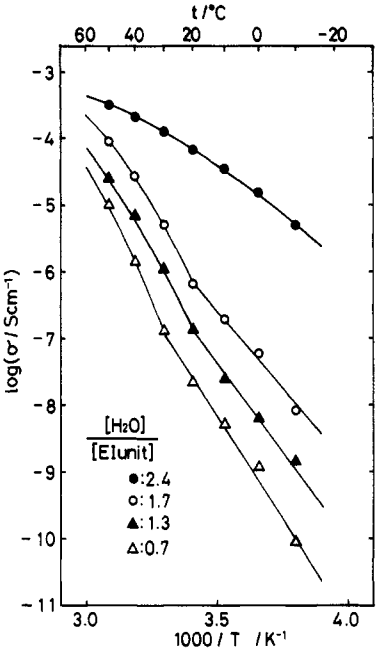

Figure 10. Arrhenius plots of ionic conductivity for cross-linked poly(ethylenimine) hydrates.

served, reflecting the fact that all of the incorporated water was crystallized. Figure 8 shows the conductivity at 30 °C against the composition. With an increase in $[H_2O]/[EI\ unit]$ from 0.5 to 1.5, the conductivity increased from 10^{-8} to 10^{-5} S cm^{-1}. Above $[H_2O]/[EI\ unit] = 1.5$ the conductivity tended to decrease.

It has been revealed that the polymer chains in the three crystalline hydrates have planar zigzag conformation.[15,16] In the hemihydrate,[15] all hydrogen bonds are of the N–H···O or N···H–O type, and there exist no water–water hydrogen bonds. The layered structure of the two-dimensional network structure of the hydrogen bonds is, thus, formed along the chain axis.[15] In contrast, water–water hydrogen bonds are formed in the sesqui- and dihydrates, which leads to the formation of the three-dimensional network structure of hydrogen bonds.[16]

The fact that the activation energy for the conduction of various hydrates coincided with that of hemihydrate implied that the hydrogen bonding network structure of N–H···O and N···H–O types played an important role for the conduction. The activation energy of 18–20 kcal/mol obtained in the present system is widely reported in protonic conductors with hydrogen bonds of the N–H···O or N···H–O type, as seen in $(NH_4)_2SO_4$ and NH_4ClO_4.[17] This activation energy was somewhat greater than 10 kcal/mol, which is observed in protonic conductors with O–H···O type hydrogen bonds, such as ice and KH_2PO_4.[17] The change in the conductivity with the water content seen in Figure 8 was very interesting in contrast to the structures of hydrates. However, the reason for taking the conductivity maximum at $[H_2O]/[EI\ unit] = 1.5$ is still not clear.

Comparison to Partially Amorphous PEI Hydrates. Figure 9 shows the profiles of DSC curves for the anhydrate and hydrates of cross-linked PEI networks. The anhydrate became amorphous by the cross-linked structure and its T_g was higher than that of linear PEI anhydrate. In the hydrates of $[H_2O]/[EI\ unit] = 0.7–1.7$, their T_g reduced to −32 °C, independent of the water content, and the endothermic shoulders, possibly corresponding to the melting of crystallites of PEI hydrates, appeared at 32–40 °C. The appearance of T_g showed that these hydrates were partially amorphous. When $[H_2O]/[EI\ unit] = 2.4$, T_g decreased again to −48 °C and there existed no other thermal transition except for that of hydration. Thus, the hydrate of $[H_2O]/[EI\ unit] = 2.4$ became amorphous again.

Figure 10 shows the temperature dependence of ionic conductivity for cross-linked PEI hydrates. The temperature profiles of the conductivity were considerably different from those of linear PEI hydrates, seen in Figure 7. The partially crystalline hydrates ($[H_2O]/[EI\ unit] = 0.7–1.7$) showed an Arrhenius type temperature profile of conductivity up to 20–30 °C and showed a Williams–Landel–Ferry (WLF) type temperature profile above those temperatures. However, apparent activation energies in the low-temperature region were larger than those seen in linear PEI hydrates. The break points corresponded to the melting points. The conductivity change in the amorphous hydrate ($[H_2O]/[EI\ unit] = 2.4$) showed WLF type profiles in the whole temperature range. From these results, the ionic conduction in these hydrates seemed to occur primarily in the amorphous region, especially in higher temperature regions in which WLF temperature profiles were observed.

The comparison of the conductivity values in these two kinds of PEI hydrates should be interesting. The conductivity values at the same composition were lower in the cross-linked PEI hydrates at 0 °C, comparable at 30 °C, and higher in the cross-linked PEI hydrates at 50 °C. Even at 50 °C, however, the conductivity of the linear PEI hydrate of $[H_2O]/[EI\ unit] = 1.5$ was comparable to that of the cross-linked hydrate.

The drastic changes in the temperature dependences of conductivity and its magnitude in both hydrates strongly suggested that the ionic conduction in linear PEI hydrates primarily occurred in their crystalline phases. It was concluded that linear PEI hydrates were crystalline ionic conductors based on polymeric materials and that the network structure of hydrogen bonds in the crystalline phases played an important role for the ionic conduction.

Registry No. PEI, 26913-06-4.

References and Notes

(1) Randin, J. P. *J. Electrochem. Soc.* **1982**, *129*, 1215.
(2) Wallace, R. A. *J. Appl. Phys.* **1971**, *42*, 3121.
(3) Wallace, R. A.; Jindal, B. K. *J. Electrochem. Soc.* **1971**, *118*, 707.
(4) Haase, R.; Sauermann, P. F.; Drücher, K. H. *Z. Phys. Chem.* **1966**, *48*, 206.

(5) Slade, R. C. T.; Hardwick, A.; Dickens, P. G. *Solid State Ionics* **1983**, *9/10*, 1093.
(6) Wright, P. V. *Br. Polym. J.* **1975**, *7*, 319.
(7) Watanabe, M.; Kanba, M.; Nagaoka, K.; Shinohara, I. *J. Polym. Sci., Polym. Phys. Ed.* **1983**, *21*, 939.
(8) Killis, A.; LeNest, J. F.; Cheradame, H.; Gandini, A. *Makromol. Chem.* **1982**, *183*, 2835.
(9) Watanabe, M.; Sanui, K.; Ogata, N. *Macromolecules* **1986**, *19*, 815.
(10) Watanabe, M.; Suzuki, A.; Santo, T.; Sanui, K.; Ogata, N. *Macromolecules* **1986**, *19*, 1921.
(11) See, for example: Farrington, G. C. *Science (Washington, D.C.)* **1979**, 204, 1371. Hagenmuller, P., Gool, W. V., Eds. *Solid Electrolytes*; Academic: New York, 1978.
(12) (a) Saegusa, T.; Ikeda, H.; Fujii, H. *Polym. J. (Tokyo)* **1972**, 3, 325; (b) *Macromolecules* **1972**, *5*, 108.
(13) Tanaka, R.; Ueoka, I.; Takaki, Y.; Kataoka, K.; Saito, S. *Macromolecules* **1983**, *16*, 849.
(14) Chatani, Y.; Kobatake, T.; Tadokoro, H.; Tanaka, R. *Macromolecules* **1982**, 15, 170.
(15) Chatani, Y.; Kobatake, T.; Tadokoro, H. *Macromolecules* **1983**, *16*, 199.
(16) Chatani, Y.; Tadokoro, H.; Saegusa, T.; Ikeda, H. *Macromolecules* **1981**, *14*, 315.
(17) See, for example: Glasser, L. *Chem. Rev.* **1975**, *75*, 21.
(18) Randin, J. P.; Viennet, R. *J. Electrochem. Soc.* **1982**, *129*, 2349.
(19) Deb, S. K. *Philos, Mag.* **1973**, *27*, 801.
(20) Mohapatra, S. K.; Boyd, G. D.; Storz, F. G.; Wagner, S.; Wudl, F. *J. Electrochem. Soc.* **1979**, *126*, 805.
(21) Mohapatra, S. K. *J. Electrochem. Soc.* **1978**, *125*, 284.
(22) Green, M.; Smith, W. C.; Weiner, J. A. *Thin Solid Films* **1976**, *38*, 89.

Photoconductivity of Donor-Loaded Polyimides

Steven C. Freilich

Central Research and Development Department, E. I. du Pont de Nemours & Company, Experimental Station, Wilmington, Delaware 19898. *Received August 4, 1986*

ABSTRACT: The addition of electron donors to Kapton polyimide film results in an enhancement of photocurrent by as much as 5 orders of magnitude as compared to the virgin polymer. The mechanism of the enhancement is the result of radiation absorption by the charge-transfer complex formed between the added electron donor and the imide portion of the polymer backbone. Excitation is followed by rapid and complete electron transfer from the donor to pyromellitimide to yield the radical anion of the polymer and the radical cation of the donor. This species undergoes rapid back electron transfer, and the geminate recombination process is examined through an Onsager model analysis.

The photoconductivity of Kapton polyimide film has been noted in the literature in recent years.[1-6] UV,[4] X-ray,[5,6] and visible radiation[1-3] have been utilized as excitation sources. Although polyimides are well-known for their high thermal stability, solvent insensitivity, and good dielectric characteristics, the low quantum yield of photocurrent generation has limited the utility of these materials as photoconductors. In this paper, a new class of films with enhanced photoconductive properties is presented, namely electron-donor-loaded polyimide films. These films are characterized by higher photocurrent gains achieved without significantly sacrificing other positive features of polyimides.

Sensitization of photoconductivity in electron-donating polymers by the addition of electron acceptors has been widely reported, with most of the focus on poly(*N*-vinylcarbazole) (PVK).[7,8] Little work has appeared in the literature concerning electron-accepting polymers and electron-donor additives. Kapton polyimide film falls into the class of electron-accepting polymers, by virtue of the pyromellitimide group in the polymer backbone.

The process of photoconductivity can be divided into three individual steps: (1) the absorption of radiation; (2) the conversion of absorbed radiation into charge carriers; (3) the transport of free charge carriers throughout the bulk of the material to create a current flow in the external circuit. This paper reports on the first two steps in the mechanism of photoconductivity of electron-donor-loaded Kapton polyimide film. Carrier transport will be addressed in a future publication.

Experimental Section

Kapton polyimide films of various thicknesses are commercially available from Du Pont. These films are largely composed of oxydianiline pyromellitic acid polyimide (PMDA–ODA), the structure of which is shown below. PMDA–ODA films produced

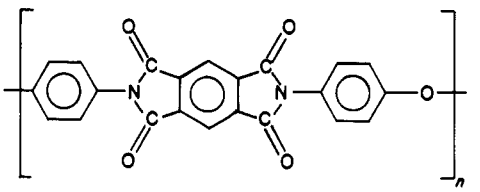

in the laboratory were generated by starting from the poly(amic acid) solution in *N,N*-dimethylacetamide (DMAC). Thus, a 12% solution of the poly(amic acid) was spin-coated onto conductive indium tin oxide coated glass (Kaufman Glass) at 2000 rpm for 1 min. Heating of the films at 90 °C for 10 min followed by immersion in a one-to-one solution of pyridine in acetic anhydride resulted in nearly complete imidization.

Electron donors were obtained from Aldrich Chemical Co. and were purified by standard techniques.

Steady-state DC photoconductivity was measured in the sandwich configuration, using an electrode arrangement consisting of a guard ring to prevent the measurement of surface charge leakage, a back electrode of silver paint, and a front electrode of conductive glass (Kaufman Glass). Current measurement was made through a picoammeter (Keithley 616) after application of a potential across the sample. Illumination was afforded by monochromatized radiation from a quartz–iodide lamp.

Photoinduced discharge measurements were made by passing the grounded film samples under a 1-mil tungsten corona wire and monitoring the change in surface potential as a function of 480-nm illumination time with an electrostatic voltmeter (Monroe Electronics). Photocurrent yield, ϕ, is obtained through the analysis $\phi = (C/eIA)(dV/dt_0)$, where C, I, A, and e are the capacitance of the film, the incident photon flux, the absorbance of the sample at the appropriate wavelength, and the electron unit of charge, respectively, and dV/dt_0 represents the measured initial slope of the voltage vs. time discharge plot.

Transient spectroscopy was performed on a Nd^{+3}:YAG laser flash photolysis apparatus with frequency doubling and tripling

0024-9297/87/2220-0973$01.50/0